TRANSIENT DYNAMIC BEHAVIOR OF TWO PHASE MAGNETO-ELECTRO-ELASTIC SENSORS BONDED TO ELASTIC RECTANGULAR PLATES

B.Biju

Department of Mechanical Engineering

M. A. College of Engineering, Kerala, 686 666, India

Email: bbiju@rediff.com

N.Ganesan

Machine Design Section, Department of Mechanical Engineering

Indian Institute of Technology Madras, Chennai 600 036, India

Email: nganesan@iitm.ac.in

K.Shankar

Machine Design Section, Department of Mechanical Engineering

Indian Institute of Technology Madras, Chennai 600 036, India

Email: skris@iitm.ac.in

Submitted: June 14, 2012 ***Accepted: Aug. 4, 2012*** ***Published: Sep. 1, 2012***

Abstract- Transient dynamic behavior of Magneto-electro-elastic (MEE) sensors bonded to a mild steel plate using 3D magnetic vector potential approach is presented. The electric field induced by time varying magnetic field is non-conservative and can be described by electric scalar potential and magnetic vector potentials. The aim of the study is to find how different volume fractions of the MEE composite behave in sensor applications at various locations on the plate subjected to different boundary conditions. The 3D plate and the sensor are modeled using eight nodded brick element with sufficient numbers of elements across the thickness direction to capture the bending behavior of the plate correctly. The four boundary conditions chosen are one symmetric boundary condition (CCCC), one free edge (CCFC), two adjacent free edges (CFFC) and two opposite free edges (FCFC). It is seen that the electric response is maximum when volume fraction v_f=0.2 for all sensor locations with different boundary conditions. The boundary conditions significantly influence the magnetic response; volume fraction v_f=0.4 gives noticeably higher values of magnetic potential in almost all the cases except for CFFC boundary condition with sensor near the edge and FCFC boundary condition with sensor at an off set distance from the edge.

Index terms*: Magneto-electro-elastic, sensor, magnetic vector potential, transient response, finite element*

I. INTRODUCTION

Smart materials which convert energy between multiple physical domains form integral part of smart and intelligent structures. Active and multifunctional smart materials having self sensing and adaptive capabilities are used to develop intelligent structures employed for applications like sensing, actuation, active control etc. Magneto-electro-elastic (MEE) materials belong to the family of smart materials; exhibit magnetic-electric-mechanical coupling effect in such a way that they produce electric and magnetic field when deformed and conversely, undergo deformation when subjected to electric and magnetic field. In addition to this, a magneto-electric coupling effect which is absent in the constituent phases is exhibited by these class of magneto-electro-elastic materials. Due to exceptional nature of these materials to convert one form of energy into another, multifunctional materials can be developed which find widespread applications in areas like magnetic field probes, acoustic devices, medical ultrasonic imaging, sensors and actuators etc. The behavior of MEE sensors bonded at different locations on an elastic base plate and the effect of boundary conditions on the dynamic response will help to

determine the best operating conditions of MEE devices which in turn will lead to emerging areas for application of magneto-electro-elastic materials as sensors and actuators.

Fibrous composites consisting of piezomagnetic cobalt iron oxide ($CoFe_2O_4$) matrix reinforced by piezoelectric barium titanate ($BaTiO_3$) fibers [1] are analyzed for the sensory response. Both phases are transversely isotropic with the axis of symmetry oriented in the z-direction. Aboudi [2] has employed a homogenization method assuming that the composites have a periodic structure, for predicting the effective moduli of magneto-electro-elastic composites. Huang and Yu [3] examined the dynamic electromechanical responses of piezoelectric rectangular plate based on the three-dimensional linear piezoelectricity. The displacements and the electric potential were expanded through the plate thickness and the responses were expressed in terms of Fourier coefficients. A mathematical model was proposed by Qing *et al.* [4] for static analysis of a hybrid laminate and dynamic analysis of a clamped aluminum plate with piezoelectric patches. The same linear quadrilateral element is used to discretize the plate and patches to account for the compatibility of generalized displacements and generalized stresses on the interface between the plate and patches. Sunar *et al.* [5] has made finite element modeling of a fully coupled thermopiezomagnetic medium using a thermodynamic potential. Sirohi *et al.* [6] investigated the piezoelectric strain sensor in which strain is measured in terms of charge developed by direct piezoelectric effect. Huang *et al.* [7] examined the dynamic electromechanical response of piezoelectric sensors and actuators which are modeled as rectangular plate and the variation of electric potential, stresses and electric displacements across the thickness were evaluated. Ghosh *et al.* [8] has presented the 3D finite element formulation of composite laminate containing magnetostrictive patches. Galopin *et al.* [9] has done finite element modeling of magneto electric sensors and the magneto electric effect stemming from piezoelectric and magnetostrictive composite was studied. Pietrzakowski *et al.* [10] dealt with active vibration control of rectangular plates containing piezoelectric sensor/actuator layers using velocity control feed back to suppress vibration. Daga *et al.* [11] has studied the behavior of MEE sensors bonded to beam under transient mechanical loading using plane stress assumption. Miniger *et al.* [12] has presented 3D finite element model of a bi-layer beam subjected to magnetic fields and subsequently developed a cylindrical magnetoelectric sensor. The transient response of a bi-layer multiferroic composite plate was studied by Wang *et al*. [13]. Biju *et al.* [14] studied the dynamic response of multiphase MEE sensors bonded to beams using magnetic vector potential approach.

The present work is an application oriented numerical study of multiphase magneto-electro-elastic composite using magnetic vector potential approach, for sensing applications. It deals with transient response of magneto-electro-elastic sensor bonded to a mild steel rectangular plate. The purpose of the sensor is to measure the electric and magnetic response to applied mechanical loading. The aim of the study is to find how different volume fractions of the composite behave in sensor applications at various locations on the plate subjected to different boundary conditions. The sensor is bonded on the top surface of the plate and three dimensional theory of elasticity is used to model the continuum. A perfect bonding between the mild steel plate and the sensor is assumed and the present study ignores the potential noise effects which come across during experiments.

Response of the sensor is studied when the plate is subjected to a time-harmonic point load excitation in transverse direction with different boundary conditions so as to investigate the influence of boundary condition on the dynamic response.These studies will be highly useful when we use MEE sensors and actuators for active vibration control of structures. Commercial finite element package ANSYS is used to validate the computer code developed for the study. ANSYS cannot model fully coupled magneto-electro-elastic materials but it can model piezoelectric PZT-5 which is used to compare the results of the code.

II THEORETICAL FORMULATION

a. Constitutive Equations

The constitutive equations for the MEE medium [5] relating stress σ_j, electric displacement D_l and magnetic field intensity H_l to strain S_k, electric field E_m and magnetic flux density B_m, exhibiting linear coupling between magnetic, electric and elastic field can be written as

$$\sigma_j = C_{jk}S_k - e_{jm}E_m - d_{jm}B_m \qquad (1,a)$$

$$D_l = e_{lj}S_k + \varepsilon_{lm}E_m + b_{ml}B_m \qquad (1,b)$$

$$H_l = -d_{lj}S_k - b_{lm}E_m + \mu_{lm}^{-1}B_m \qquad (1,c)$$

where C_{jk}, ε_{lm} and μ_{lm} are elastic, dielectric and magnetic permeability coefficients respectively and e_{jl}, d_{jl} and b_{lm} are the piezoelectric, piezomagnetic and magneto electric material coefficients. ($d_{jl} = q_{jl}\mu_{lm}^{-1}$ and $b_{lm} = m_{lm}\mu_{lm}^{-1}$) Here $j,k = 1,\ldots,6$ and $l,m = 1,..,3$.

Table1 Material properties of PZT-5 and different volume fraction v_f of multiphase magneto-electro-elastic $BaTiO_3$-$CoFe_2O_4$ [2, 11, 15]

	0.0 *vf*	0.2 *vf*	0.4 *vf*	0.6 *vf*	0.8 *vf*	1.0 *vf*	PZT-5
Elastic constants							
$C_{11}=C_{22}$	286	250	225	200	175	166	99.2
C_{12}	173	146	125	110	100	77	54.01
$C_{13}=C_{23}$	170	145	125	110	100	78	50.77
C_{33}	269.5	240	220	190	170	162	86.85
$C_{44}=C_{55}$	45.3	45	45	45	50	43	21.1
Piezoelectric constants							
$e_{31}=e_{32}$	0	-2	-3.0	-3.5	-4.0	-4.4	-7.20
e_{33}	0	4	7.0	11.0	14.0	18.6	15.11
$e_{24}=e_{15}$	0	0	0	0	0	11.6	12.32
Dielectric constants							
$\varepsilon_{11} = \varepsilon_{22}$	0.08	0.33	0.8	0.9	1.0	11.2	1.53
ε_{33}	0.093	2.5	5.0	7.5	10	12.6	1.5
Magnetic permeability constants							
$\mu_{11} = \mu_{22}$	-5.9	-3.9	-2.5	-1.5	-0.8	0.05	0
μ_{33}	1.57	1.33	1.0	0.75	0.5	0.1	0
Piezomagnetic constants							
$q_{31}=q_{32}$	580	410	300	200	100	0	0
q_{33}	700	550	380	260	120	0	0
$q_{24}=q_{15}$	560	340	220	180	80	0	0
Magnetoelectric constants							
$m_{11}=m_{22}$	0	2.8	4.8	6.0	6.8	0	0
m_{33}	0	2000	2750	2500	1500	0	0
Density							
ρ	5300	5400	5500	5600	5700	5800	7750

C_{jk} in $10^9 N/m^2$, e_{lj} in C/m^2, ε_{lm} in $10^{-9} C/Vm$, q_{lj} in N/Am, μ_{lm} in $10^{-4} Ns^2/C^2$, m_{lm} in $10^{-12} Ns/VC$, ρ in kg/m^3

The dynamic potential G for the magneto-electro-elastic medium can be written as

$$G = \frac{1}{2} S^T C S - \frac{1}{2} E^T \varepsilon E + \frac{1}{2} B^T \mu^{-1} B - S^T e E - S^T l B - B^T b E \qquad (2)$$

b. Differential equation for magneto-electro-elastic medium

The energy functional π neglecting surface tractions [5] can be written as

$$\pi = \int_v G \; dv - \int_v u^T P_b \; dv + \int_v \phi \; \rho_v dv - \int_v A^T J \; dv \qquad (3)$$

where u, ϕ, A are mechanical displacement, electric scalar potential and magnetic vector potential respectively. P_b, ρ_v and J are the body force, free charge density and total current vector respectively.

The generalized Hamilton principle has the form

$$\delta \int_{t_1}^{t_2} (T - \pi) dt = 0 \qquad (4)$$

where T is the kinetic energy.

$$T = \int_v \frac{1}{2} \rho \dot{u}^T \dot{u} \; dv \qquad (5)$$

$$\delta G = \delta S^T \sigma - \delta E^T D + \delta B^T H \qquad (6)$$

$$\delta \int_{t_1}^{t_2} (T - \pi) dt = \int_{t_1}^{t_2} dt [\int_v (-\rho \delta u^T \ddot{u} - \delta S^T \sigma + \delta E^T D - \delta B^T H + \delta u^T P_b - \delta \phi^T \rho_v + \delta A^T J) dv] = 0 \qquad (7)$$

Equation (7) can be rewritten as

$$\int_{t_1}^{t_2} dt [\int_v \delta u^T (-\rho \ddot{u} + L_u^T \sigma + P_b) dv + \int_v \delta \phi^T (\nabla^T D - \rho_v) dv + \int_v \delta A^T (\dot{D} - \nabla X H + J) dv] = 0 \qquad (8)$$

Accordingly the following equations with appropriate boundary conditions must be satisfied for a magneto-electro-elastic medium.

$$-\rho \ddot{u} + L_u^T \sigma + P_b = 0 \qquad (9,a)$$

$$\nabla^T D - \rho_v = 0 \qquad (9,b)$$

$$\dot{D} - \nabla X H + J = 0 \qquad (9,c)$$

where equation (9,a) is the equation of motion for the mechanical field and equations (9,b) and (9,c) are the Maxwell's equations for the electric and the magnetic fields.

c. Finite element modeling using vector potential

The displacements $\{u\} = \{u_x\, u_y\ \ u_z\}^T$, electric potential (ϕ) and magnetic potentials $\{A\} = \{A_x\, A_y\ \ A_z\}^T$ within the element can be expressed in terms of suitable shape functions.

$$\{u\} = [N_u]\{u^e\}\,;\phi = [N_\phi]\{\phi^e\}\ ;\ \{A\} = [N_A]\{A^e\} \qquad (10)$$

An eight nodded isoparametric element having the following shape function is used.

$$N_i(\xi,\eta,\tau) = \frac{1}{8}(1+\xi\xi_i)(1+\eta\eta_i)(1+\tau\tau_i) \quad \text{i =1, 2..., 8} \qquad (11)$$

where ξ , η and τ are the natural coordinates.

The strains can be related to the nodal degree of freedom by the following expression

$$\{S\} = [B_u]\{u^e\} \qquad (12)$$

where $[B_u]$, the strain displacement matrix can be written as

$$[B_u] = [L_u][N_u] \qquad (13)$$

$$[B_u] = \begin{bmatrix} \frac{\partial N_1}{\partial x} & 0 & 0 & .... \\ 0 & \frac{\partial N_1}{\partial y} & 0 & .... \\ 0 & 0 & \frac{\partial N_1}{\partial z} & .... \\ \frac{\partial N_1}{\partial y} & \frac{\partial N_1}{\partial x} & 0 & .... \\ 0 & \frac{\partial N_1}{\partial z} & \frac{\partial N_1}{\partial y} & .... \\ \frac{\partial N_1}{\partial z} & 0 & \frac{\partial N_1}{\partial x} & .... \end{bmatrix} \qquad (14)$$

Recalling the Maxwell's relations

$$E = -\nabla\phi - \dot{\mathrm{A}} \qquad (15,a)$$

$$B = \nabla \times A \qquad (15,b)$$

In Cartesian coordinates

$$\nabla \times A = \hat{\mathrm{i}}\ (\frac{\partial A_z}{\partial y} - \frac{\partial A_y}{\partial z}) + \hat{\mathrm{j}}\ (\frac{\partial A_x}{\partial z} - \frac{\partial A_z}{\partial x}) + \hat{\mathrm{k}}\ (\frac{\partial A_y}{\partial x} - \frac{\partial A_x}{\partial y}) \qquad (16)$$

The electric field vector can be expressed as

$$\begin{Bmatrix} E_x \\ E_y \\ E_z \end{Bmatrix} = \begin{Bmatrix} -\dfrac{\partial \phi}{\partial x} \\ -\dfrac{\partial \phi}{\partial y} \\ -\dfrac{\partial \phi}{\partial z} \end{Bmatrix} - \begin{Bmatrix} \dot{A}_x \\ \dot{A}_y \\ \dot{A}_z \end{Bmatrix} \qquad (17)$$

The electric field vector can be related to the electric potential as a nodal degree of freedom using the following expression as

$$\{E\} = -[\nabla N_\phi]\ \phi_e - [N_A]\{\dot{A}_e\}$$

$$= \left[B_\phi\right]\left\{\phi^e\right\} - [N_A]\{\dot{A}_e\} \qquad (18)$$

The derivative of shape function matrix $[B_\phi]$ matrix is given below as

$$[B_\phi] = [L_\phi][N_\phi]$$

$$[B_\phi] = \begin{bmatrix} -\dfrac{\partial N_1}{\partial x} & -\dfrac{\partial N_2}{\partial x} & \cdots & -\dfrac{\partial N_8}{\partial x} \\ -\dfrac{\partial N_1}{\partial y} & -\dfrac{\partial N_2}{\partial y} & \cdots & -\dfrac{\partial N_8}{\partial y} \\ -\dfrac{\partial N_1}{\partial z} & -\dfrac{\partial N_2}{\partial z} & \cdots & -\dfrac{\partial N_8}{\partial z} \end{bmatrix} \qquad (19)$$

The magnetic flux density vector can be expressed as

$$\begin{Bmatrix} B_x \\ B_y \\ B_z \end{Bmatrix} = \begin{Bmatrix} \dfrac{\partial A_z}{\partial y} - \dfrac{\partial A_y}{\partial z} \\ \dfrac{\partial A_x}{\partial z} - \dfrac{\partial A_z}{\partial x} \\ \dfrac{\partial A_y}{\partial x} - \dfrac{\partial A_x}{\partial y} \end{Bmatrix} \qquad (20)$$

The magnetic field vector can be related to the magnetic vector potentials as nodal degrees of freedom using the following expression as

$$\{B\} = [B_A]\{A_e\} \qquad (21)$$

where $[B_A] = [L_A][N_A]$

$$= \begin{bmatrix} 0 & -\frac{\partial N_1}{\partial z} & \frac{\partial N_1}{\partial y} & \dots \\ \frac{\partial N_1}{\partial z} & 0 & -\frac{\partial N_1}{\partial x} & \dots \\ -\frac{\partial N_1}{\partial y} & \frac{\partial N_1}{\partial x} & 0 & \dots \end{bmatrix} \qquad (22)$$

d. Evaluation of Elemental Matrices

The finite element equations for MEE solid can be written as

$$\begin{aligned} &[M^e_{uu}]\{\ddot{u}^e\} + [C^e_{uA}]\{\dot{A}^e\} + [K^e_{uu}]\{u^e\} + [K^e_{u\phi}]\{\phi^e\} - [K^e_{uA}]\{A^e\} = \{F^e\} \\ &[C^e_{\phi A}]\{\dot{A}^e\} + [K^e_{\phi u}]\{u^e\} - [K^e_{\phi\phi}]\{\phi^e\} + [K^e_{\phi A}]\{A^e\} = \{G^e\} \\ &-[K^e_{Au}]\{u^e\} + [K^e_{A\phi}]\ \{\phi^e\} + [K^e_{AA}]\{A^e\} = \{M^e\} \end{aligned} \qquad (23)$$

where $\{F\}, \{G\}$ and $\{M\}$ corresponds to elemental load vectors of applied mechanical force, electric charge and magnetic current respectively.

Different elemental matrices in Equation (23) are defined as

$$\begin{aligned} [M^e_{uu}] &= \int_v [N_u]^T [\rho][N_u] dxdydz \\ [C^e_{uA}] &= \int_v [B_u]^T [e][N_A] dxdydz \\ [C^e_{\phi A}] &= \int_v [B_\phi]^T [\varepsilon][N_A] dxdydz \\ [K^e_{uu}] &= \int_v [B_u]^T [C][B_u] dxdydz \\ [K^e_{u\phi}] &= \int_v [B_u]^T [e][B_\phi] dxdydz \\ [K^e_{uA}] &= \int_v [B_u]^T [d][B_A] dxdydz \\ [K^e_{\phi\phi}] &= \int_v [B_\phi]^T [\varepsilon][B_\phi] dxdydz \\ [K^e_{AA}] &= \int_v [B_A]^T [\mu]^{-1} [B_A] dxdydz \\ [K^e_{\phi A}] &= \int_v [B_\phi]^T [b][B_A] dxdydz \end{aligned} \qquad (24)$$

e. Solution technique for system of equations

The system of equations is solved using Newmark-beta implicit method. The damping is assumed to be proportional damping and the damping matrix is derived as

$$[C_{uu}] = \alpha\,[M_{uu}] + \beta\,[K_{uu}] \qquad (25)$$

where α , β are the proportional damping coefficients depending on natural frequencies of the structure. When electric and magnetic loading are absent, for transient mechanical loading Equation (23) can be written in coupled form as

$$\begin{bmatrix} M_{uu} & 0 & 0 \\ 0 & 0 & 0 \\ 0 & 0 & 0 \end{bmatrix} \begin{Bmatrix} \ddot{u} \\ \ddot{\phi} \\ \ddot{A} \end{Bmatrix} + \begin{bmatrix} C_{uu} & 0 & C_{uA} \\ 0 & 0 & -C_{\phi A} \\ 0 & 0 & 0 \end{bmatrix} \begin{Bmatrix} \dot{u} \\ \dot{\phi} \\ \dot{A} \end{Bmatrix} + \begin{bmatrix} K_{uu} & K_{u\phi} & -K_{uA} \\ K_{\phi u} & -K_{\phi\phi} & K_{\phi A} \\ -K_{Au} & K_{A\phi} & K_{AA} \end{bmatrix} \begin{Bmatrix} u \\ \phi \\ A \end{Bmatrix} = \begin{Bmatrix} F(t) \\ 0 \\ 0 \end{Bmatrix} \qquad (26)$$

Equation (26) can be used to evaluate the transient response of MEE continuum.

III RESULTS AND DISCUSSIONS

The plate is modelled with 8 node isoparametric element with sufficient numbers of elements across the thickness direction to capture the bending behavior of the plate correctly**.** The dimensions of the 3D plate used for the analysis are 0.3x0.3x0.006m. The dimensions of the sensor are 0.05x0.05x0.003m.The plate is subjected to a time-harmonic point load excitation of 1N in transverse direction with CCCC, CCFC, CFFC and FCFC boundary conditions (where C stands for clamped and F for free boundary condition) so as to investigate the influence of boundary condition on comparative studies. The four boundary conditions chosen are one symmetric boundary condition (CCCC), one free edge (CCFC), two adjacent free edges (CFFC) and two opposite free edges (FCFC). The approximate location of the point excitation is chosen based on the mode shape of the plate for different boundary conditions. The location of excitation and response is chosen in such a way that it does not lie on any nodal line of all the modes in the selected frequency range.

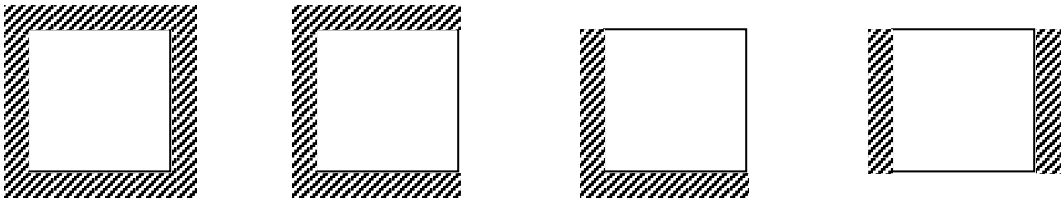

CCCC CCCF CFFC FCFC

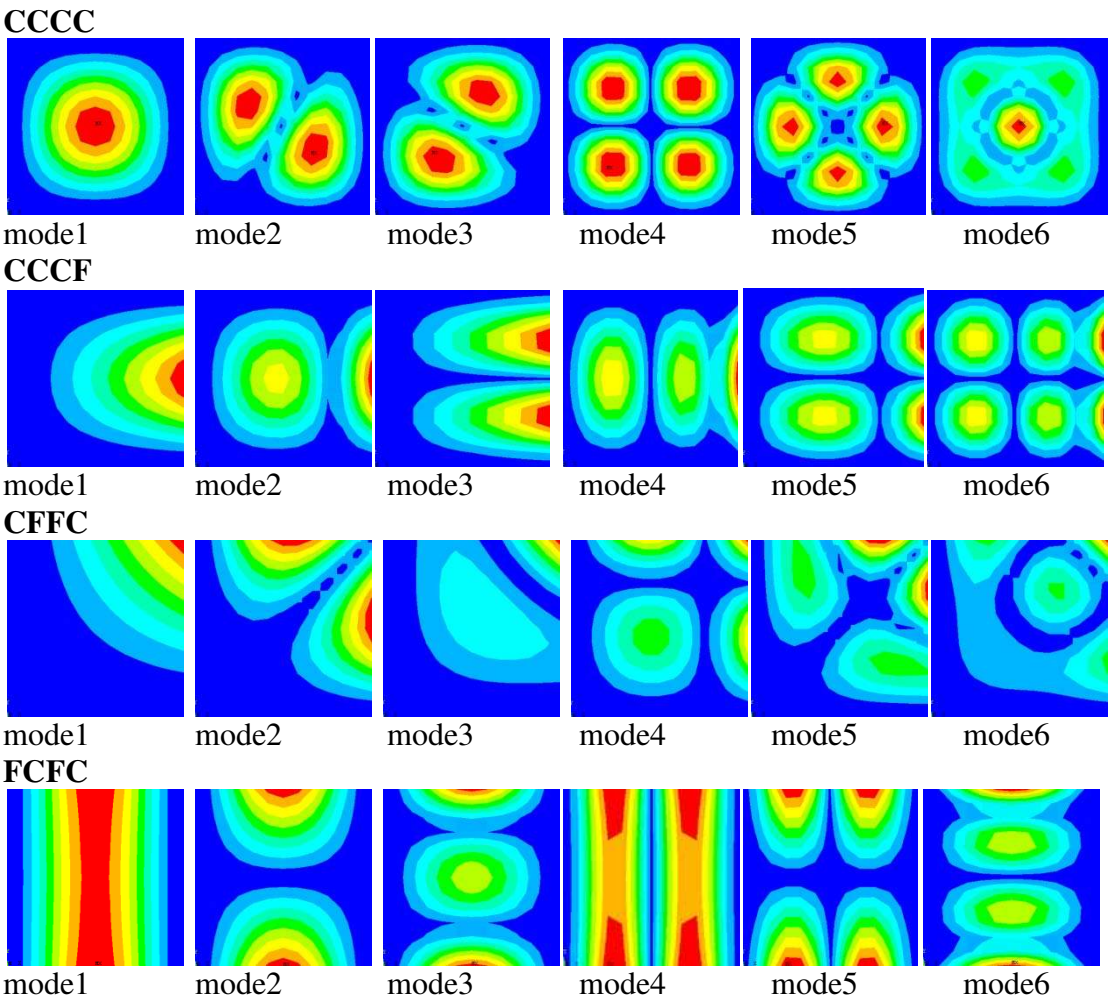

Fig 1 The different boundary conditions of the mild steel plate with associated first six mode shapes (red colour: maximum, dark blue: zero displacement other colours in between)

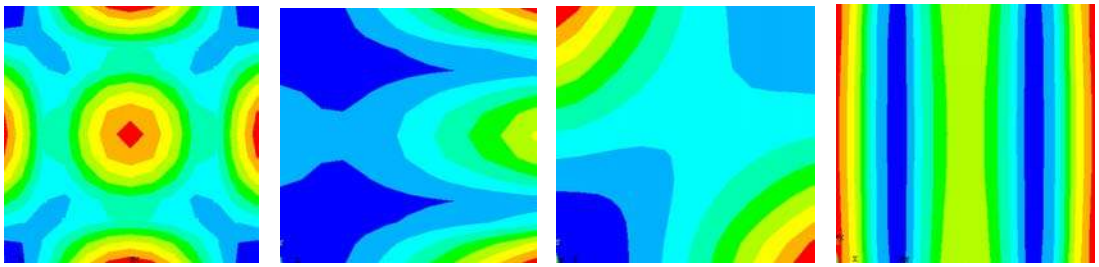

Fig 2 The Von Mises strain associated with the first mode of the structure for different boundary conditions

A schematic diagram of the four boundary condition of the mild steel plate considered for investigating the sensor response and the associated first six mode shapes of the plate is shown in

Fig 1. The response of the sensor is dependent on the strain developed in the base structure. The Von Mises strain in the base plate associated with the first mode of the structure for different boundary conditions shown in Fig 2 will be an indicative of the dependence of the sensor location on electromagnetic response. The finite element discretization of the mild steel plate with sensor bonded at three different locations with loading direction is shown in Fig 3.

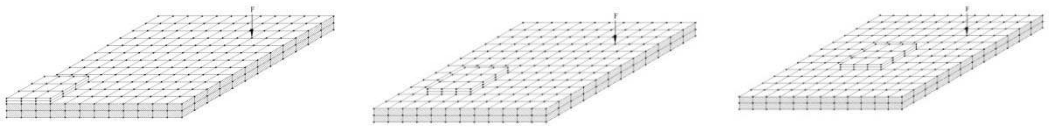

(a) (b) (c)

Fig 3 Finite element discretization of the mild steel plate with sensor bonded (a) near edge (b) off set of 0.075m and (c) at middle.

a. Validation

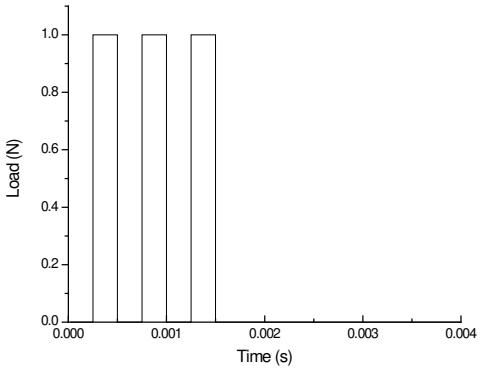

Fig 4 Load cycle for transient dynamic analysis

A computer code has been developed to study the response of magneto-electro-elastic sensor bonded on the top surface of a mild steel plate while the plate is subjected to dynamic loading. The load cycle for transient dynamic analysis is shown in Fig 4. A rectangular wave made up of a fundamental frequency and its combined odd and even harmonics is used as the load cycle. The electric and magnetic potentials are assumed zero at the clamped end.The mild steel plate will be

one electrode which will be grounded and the other electrode will be kept on the top of the sensor patch. The average acceleration criterion is used while implementing the Newmark-beta implicit method. The computer code developed has been validated for piezoelectric material model, without considering piezomagnetic coupling using the commercial finite element package ANSYS. The axial (u_x), transverse y-direction (u_y), transverse z-direction (u_z) displacements and electric potential (ϕ) of a node on the sensor which gives maximum electric response is plotted in Fig 5 using both the code and ANSYS when the plate is subjected to CCCC boundary condition. It is seen that the results are in good agreement and hence the present code is used to study the transient dynamic response of MEE sensors.

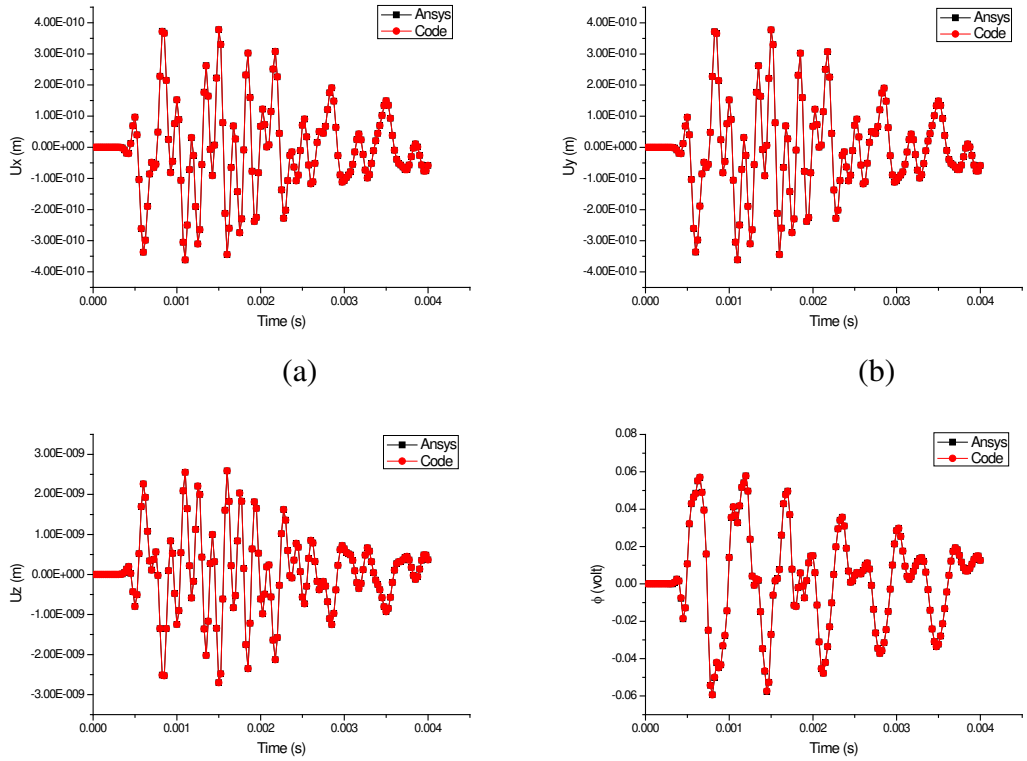

Fig 5 Validation of the code for (a) axial (u_x), (b) transverse y-direction (u_y), (c) transverse z-direction (u_z) displacements and (d) electric potential (ϕ)

b. CCCC boundary condition of the plate

Sensor near the edge

Fig 6 shows the longitudinal x-direction component (A_x), y-direction component (A_y), transverse component (A_z) of magnetic vector potential and the electric potential (ϕ) when sensor is placed near the edge with CCCC boundary condition.A node on the sensor which gives maximum response is chosen for showing the results. It is seen that the electric potential (ϕ) is maximum when volume fraction $v_f = 0.2$ which can be attributed to the induced strain because of the high elastic constants for $v_f = 0.2$. The transverse direction component of magnetic vector potential (A_z) is maximum when $v_f = 0.0$ which corresponds to pure piezomagnetic composite having maximum values of piezomagnetic coupling constants. Volume fraction $v_f = 0.4$ gives noticeably higher values of magnetic potential in the longitudinal x-direction and y-direction which can be attributed to high value of magneto electric coupling constant in the polarization direction.

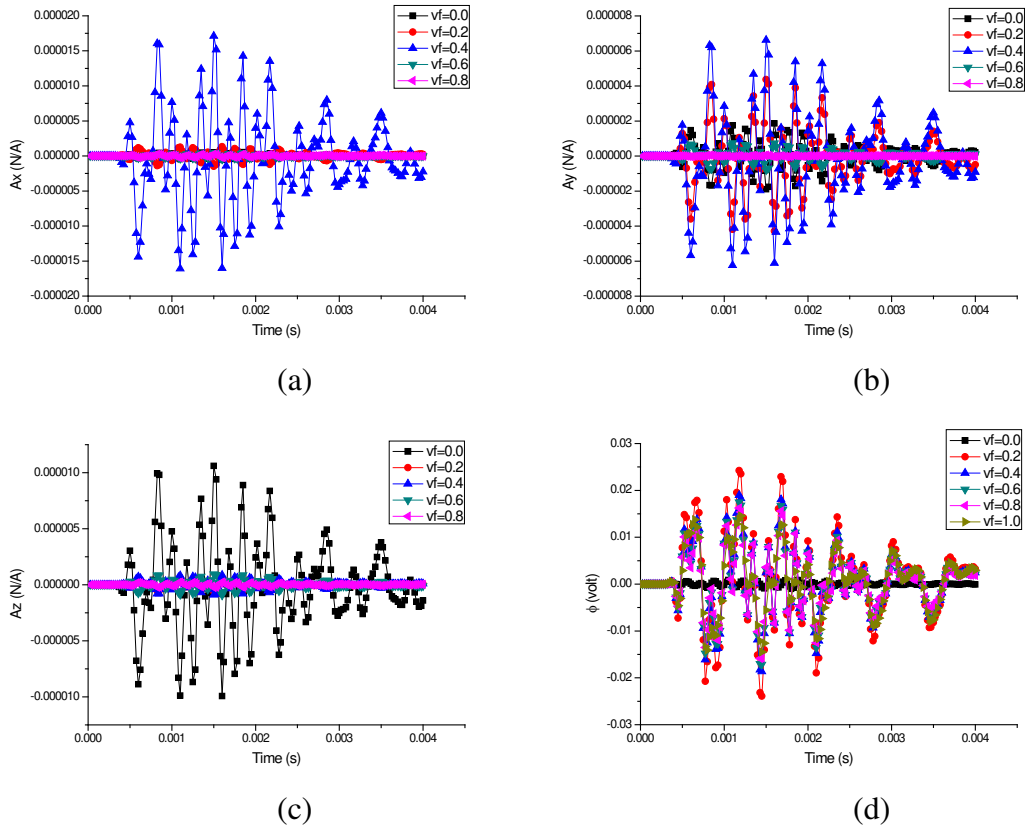

Fig 6 (a) Longitudinal x-direction component (A_x) (b) y-direction component (A_y), (c) transverse component (A_z) of magnetic vector potential and (d) electric potential (ϕ) when sensor is placed near the edge. (CCCC boundary condition)

Sensor at an off set of 0.075m

The longitudinal x-direction component (A_x), y-direction component (A_y), transverse component (A_z) of magnetic vector potential and the electric potential (ϕ) when the sensor is placed at an off set of 0.075m from the edge with CCCC boundary condition is shown in Fig 7. The maximum magnetic potential in transverse direction is for volume fraction $v_f = 0.4$ which can be attributed to high value of magneto electric coupling constant in the polarization direction. As the sensor is moved from the clamped end, the piezomagnetic coupling effect is reduced and the magneto electric effect becomes more significant. Volume fraction $v_f = 0.2$ gives noticeably higher values of magnetic potential in longitudinal x- direction and y-direction owing to the high electric potential induced in the piezoelectric phase.

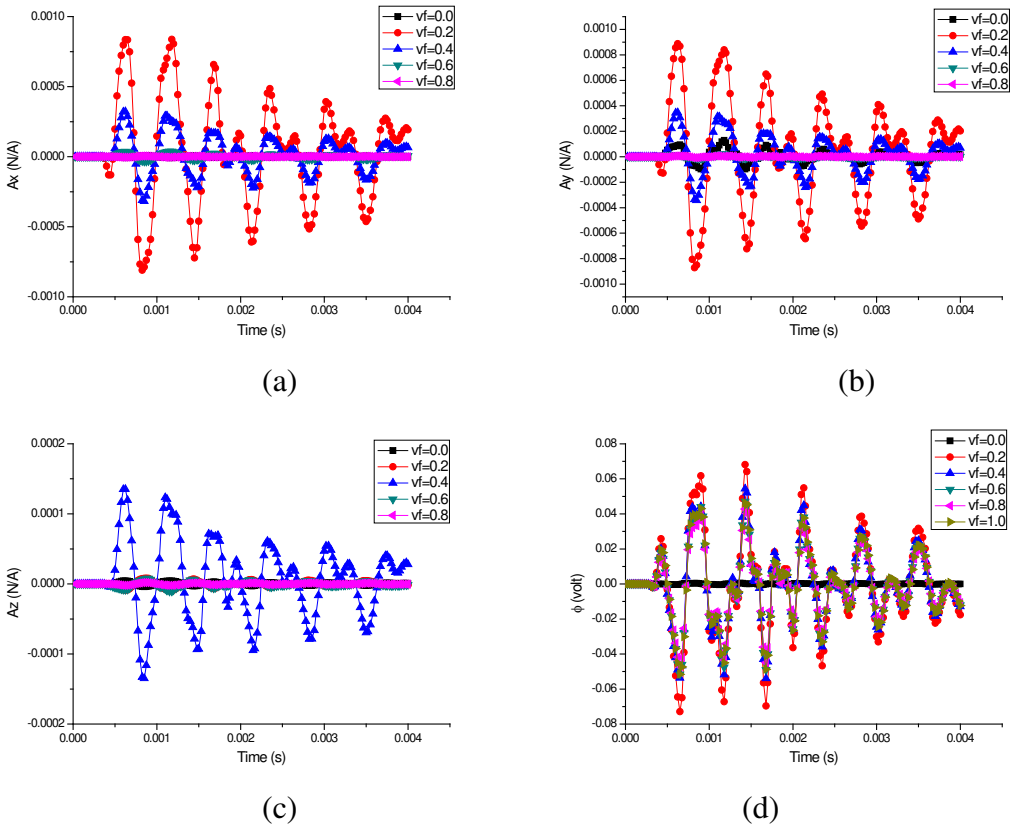

Fig 7 (a) Longitudinal x-direction component (A_x) (b) y-direction component (A_y), (c) transverse component (A_z) of magnetic vector potential and (d) electric potential (ϕ) when sensor is placed at an off set of 0.075m. (CCCC boundary condition)

Sensor at the centre

Fig 8 shows the longitudinal x-direction component (A_x), y-direction component (A_y), transverse component (A_z) of magnetic vector potential and the electric potential (ϕ) when sensor is placed at the centre with CCCC boundary condition. Volume fraction v_f =*0.4* having maximum magneto electric coupling constant in the polarization direction show maximum magnetic potential in longitudinal x-direction and y-direction. The transverse direction component of magnetic potential is high for v_f =*0.6* of the composite.

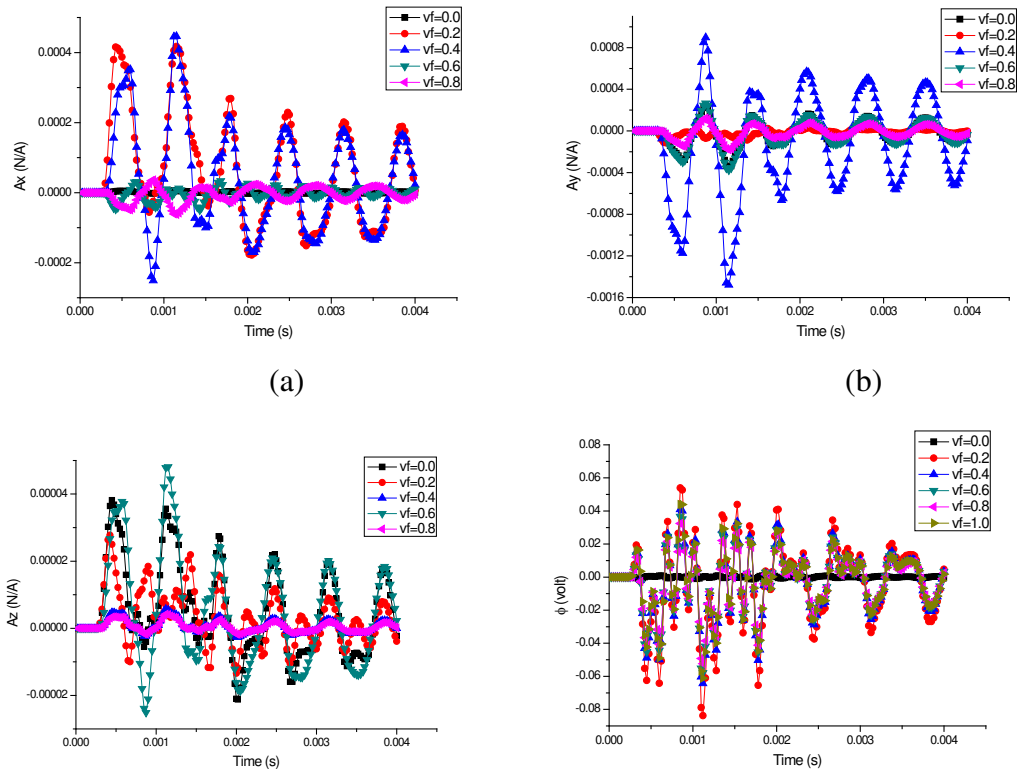

Fig 8 (a) Longitudinal x-direction component (A_x) (b) y-direction component (A_y), (c) transverse component (A_z) of magnetic vector potential and (d) electric potential (ϕ) when sensor is placed at the centre. (CCCC boundary condition)

c. CCCF boundary condition of the plate

Sensor near the edge

Fig 9 shows the longitudinal x-direction component (A_x), y-direction component (A_y), transverse component (A_z) of magnetic vector potential and the electric potential (ϕ) when sensor is placed near the edge with CCCF boundary condition. The electric potential (ϕ) is maximum when volume fraction v_f *=0.2* for this boundary condition also. It is interesting to notice that the maximum magnetic potential in longitudinal x-direction and y-direction is for volume fraction v_f *=0.6.* The transverse component of magnetic potential is randomly fluctuating because of the influence of higher harmonics in the system response.

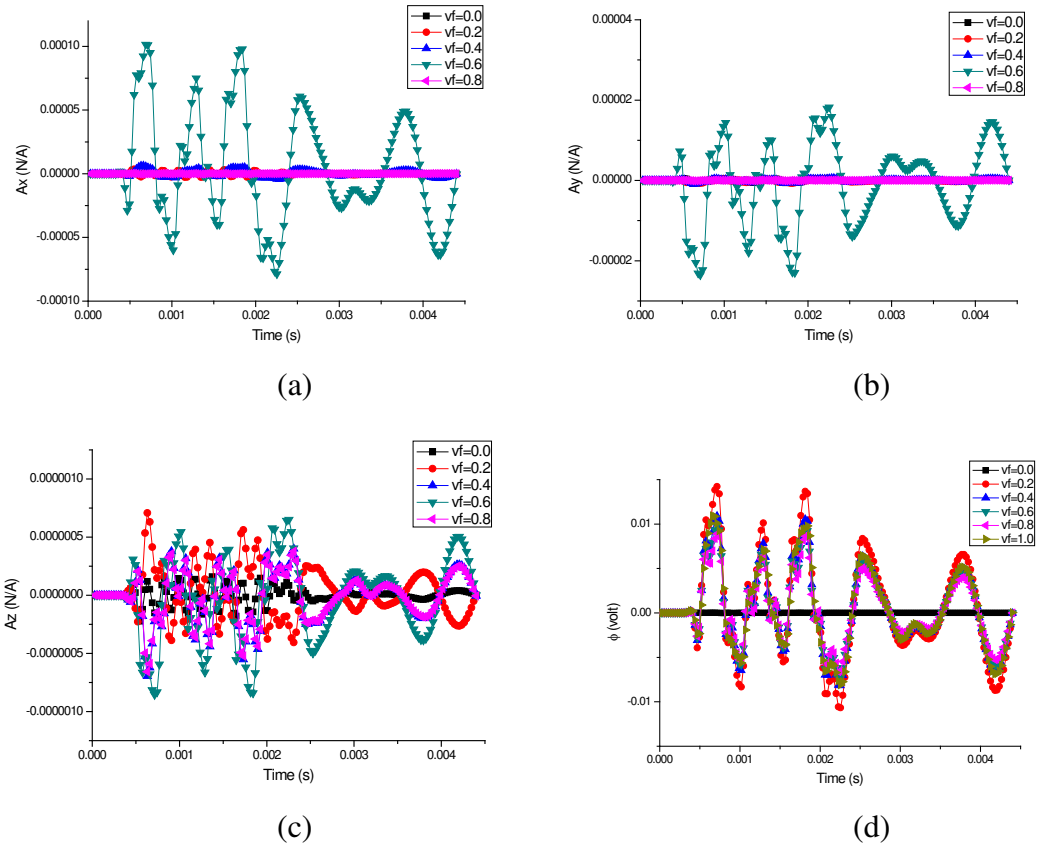

Fig 9 (a) Longitudinal x-direction component (A_x) (b) y-direction component (A_y), (c) transverse component (A_z) of magnetic vector potential and (d) electric potential (ϕ) when sensor is placed near the edge. (CCCF boundary condition)

Sensor at an off set of 0.075m

The longitudinal x-direction component (A_x), y-direction component (A_y), transverse component (A_z) of magnetic vector potential and the electric potential (ϕ) when the sensor is placed at an off set of 0.075m from the edge with CCCF boundary condition is shown in Fig 10. The longitudinal x-direction component is maximum for volume fraction v_f *=0.0* which is pure piezomagnetic phase of the composite. Volume fraction v_f *=0.4* having maximum magneto electric coupling constant in the polarization direction show maximum magnetic potential both in longitudinal y-direction and transverse direction. The transverse direction response for v_f *=0.6* is out of phase compared to other volume fractions of the composite.

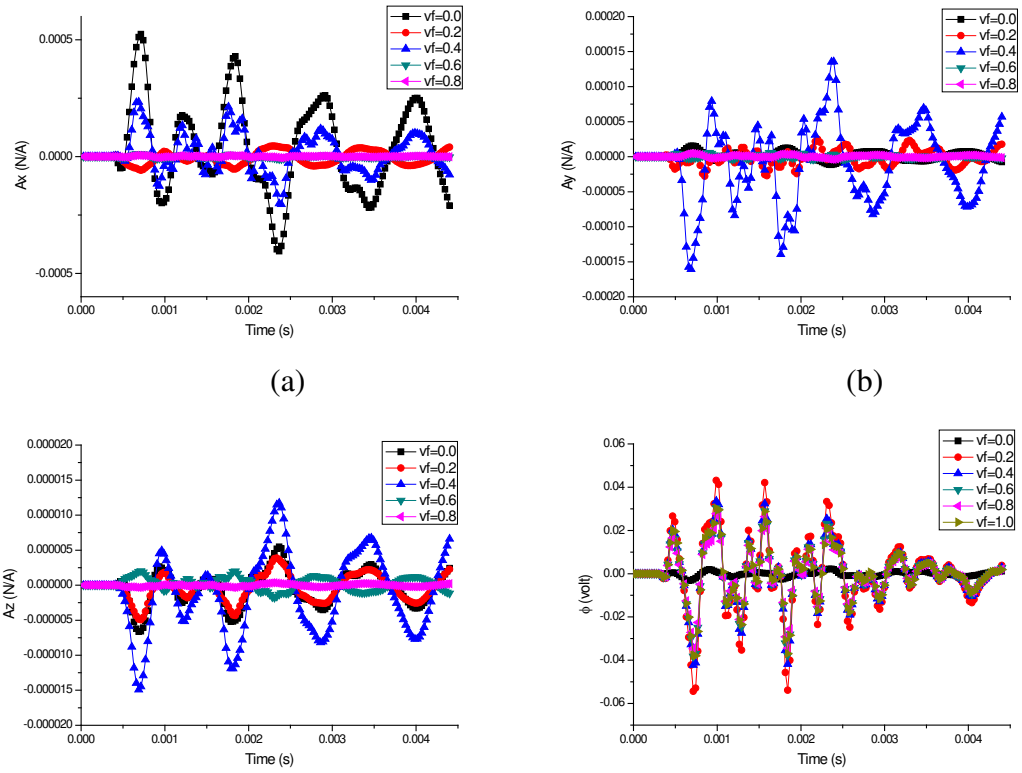

Fig 10 (a) Longitudinal x-direction component (A_x) (b) y-direction component (A_y), (c) transverse component (A_z) of magnetic vector potential and (d) electric potential (ϕ) when sensor is placed at an off set of 0.075m. (CCCF boundary condition)

Sensor at the centre

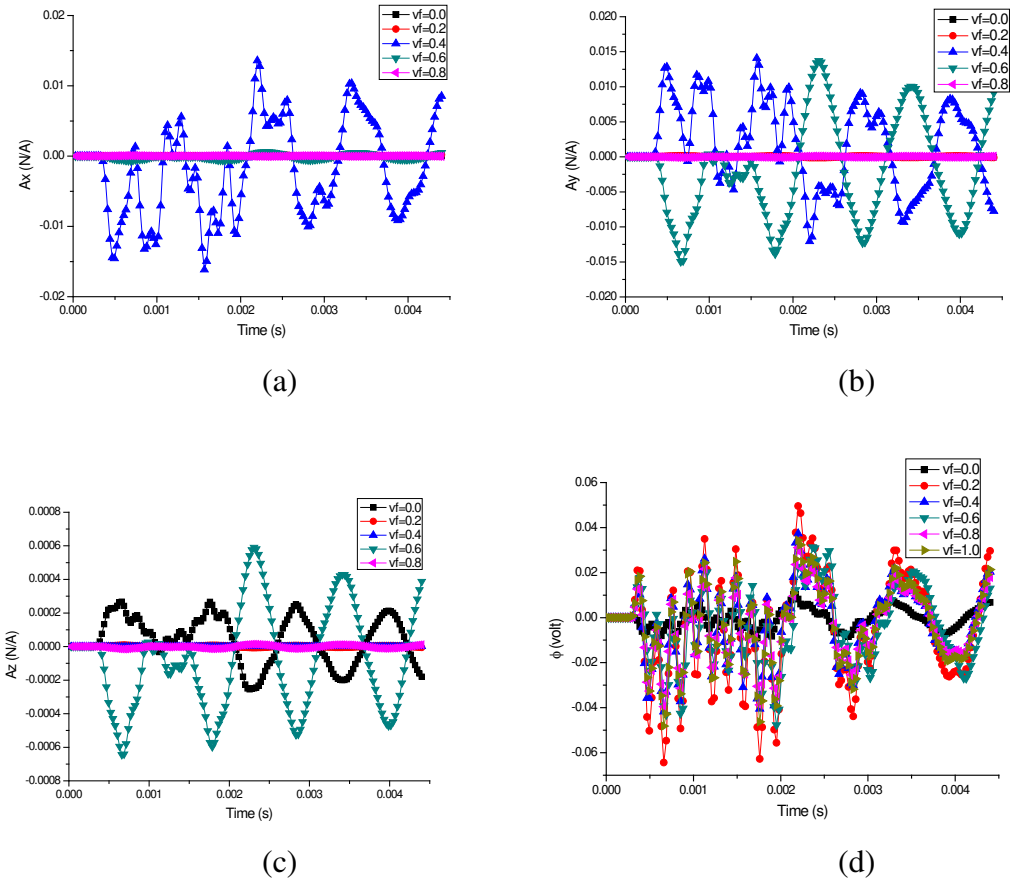

Fig 11 (a) Longitudinal x-direction component (A_x) (b) y-direction component (A_y), (c) transverse component (A_z) of magnetic vector potential and (d) electric potential (ϕ) when sensor is placed at the centre. (CCCF boundary condition)

Fig 11 shows the longitudinal x-direction component (A_x), y-direction component (A_y), transverse component (A_z) of magnetic vector potential and the electric potential (ϕ) when sensor is placed at the centre with CCCF boundary condition**.** The decay in response is very slow compared to other positions of the sensor due to the influence of higher harmonics. Both longitudinal y-direction and the transverse direction response for $v_f = 0.6$ is out of phase compared to other volume fractions of the composite. The electric potential response becomes noisy when the sensor patch is placed at the centre of a CCCF plate. The reason may be the influence of transverse component of strain which is found maximum at the centre during the first mode of vibration of the base plate.

d. CFFC boundary condition of the plate

Sensor near the edge

Fig 12 shows the longitudinal x-direction component (A_x), y-direction component (A_y), transverse component (A_z) of magnetic vector potential and the electric potential (ϕ) when sensor is placed near the edge with CFFC boundary condition. Volume fraction v_f *=0.2* gives noticeably higher values of magnetic potential in longitudinal x- direction and y-direction owing to the high electric potential induced in the piezoelectric phase. The transverse direction component of magnetic potential for volume fraction v_f *=0.0* is showing a phase shift compared to other volume fractions.

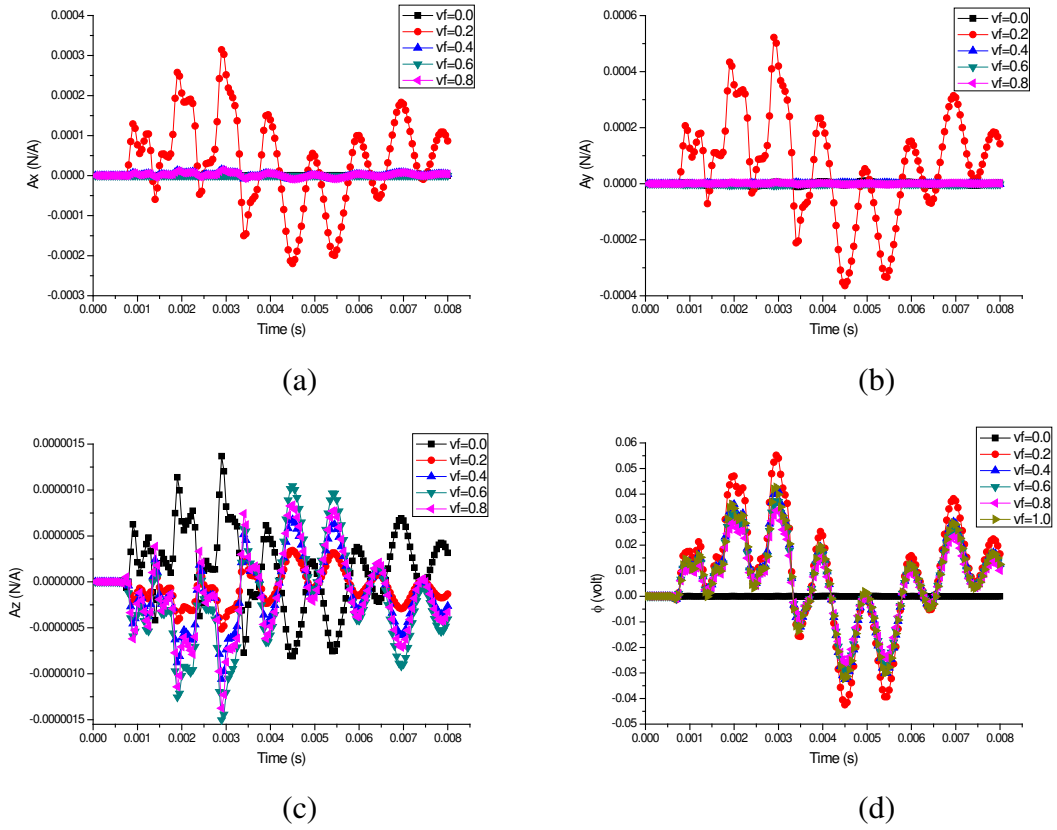

Fig 12 (a) Longitudinal x-direction component (A_x) (b) y-direction component (A_y), (c) transverse component (A_z) of magnetic vector potential and (d) electric potential (ϕ) when sensor is placed near the edge. (CFFC boundary condition)

Sensor at an off set of 0.075m

The longitudinal x-direction component (A_x), y-direction component (A_y), transverse component (A_z) of magnetic vector potential and the electric potential (ϕ) when the sensor is placed at an off set of 0.075m from the edge with CFFC boundary condition is shown in Fig 13. The longitudinal x-direction and y-direction response is noisy for volume fraction v_f =*0.2* during the initial transient owing to the noisy electric response during that period. Both longitudinal x-direction and y-direction response for v_f =*0.4* is out of phase compared to other volume fractions of the composite.

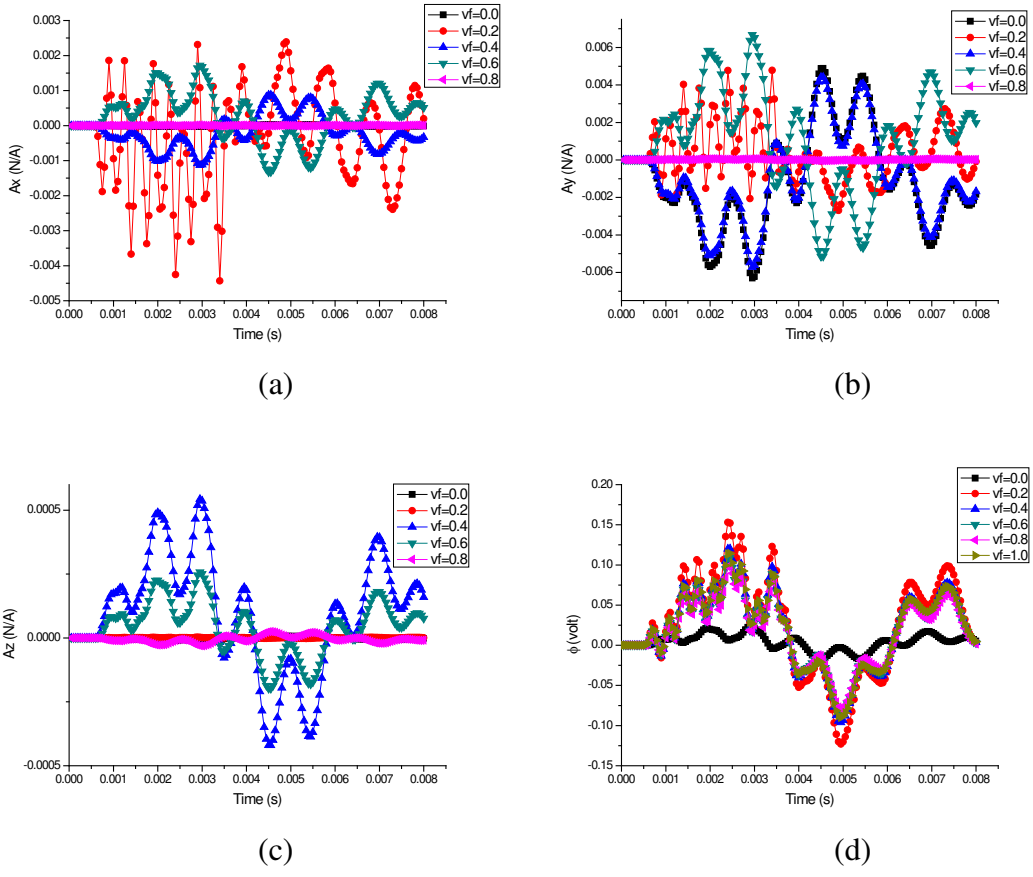

Fig 13 (a) Longitudinal x-direction component (A_x) (b) y-direction component (A_y), (c) transverse component (A_z) of magnetic vector potential and (d) electric potential (ϕ) when sensor is placed at an off set of 0.075m. (CFFC boundary condition)

Sensor at the centre

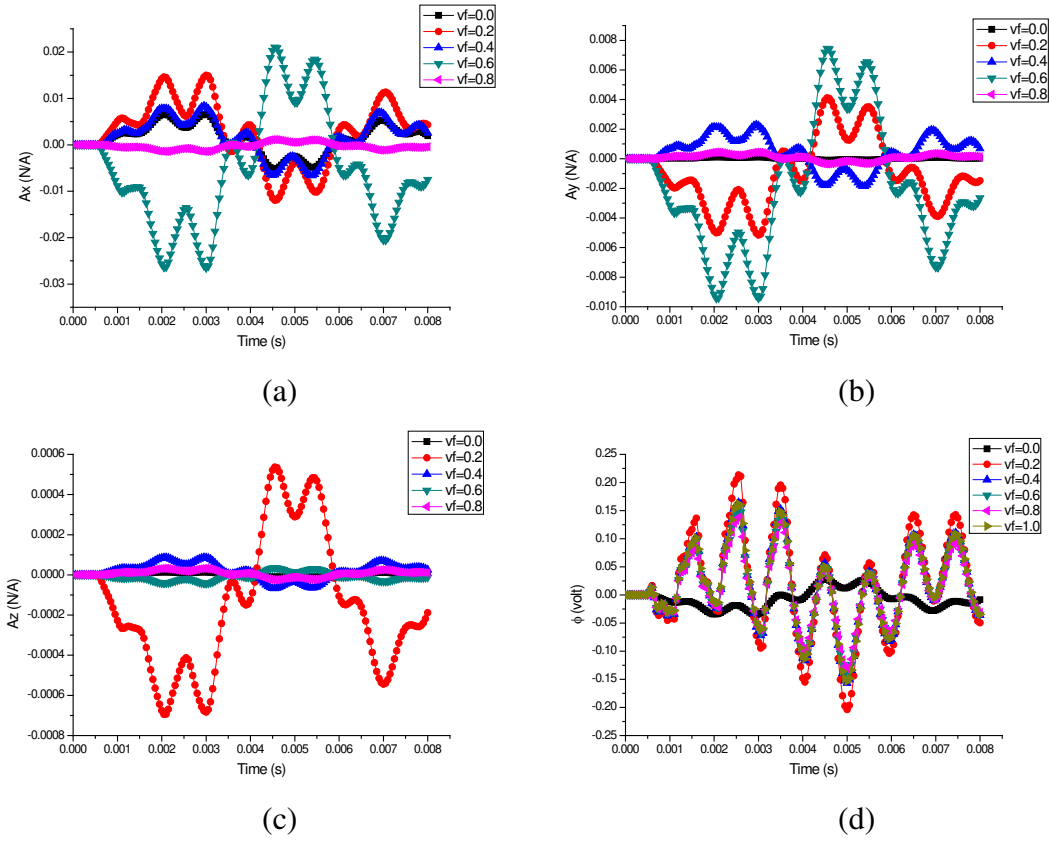

Fig 14 (a) Longitudinal x-direction component (A_x) (b) y-direction component (A_y), (c) transverse component (A_z) of magnetic vector potential and (d) electric potential (ϕ) when sensor is placed at the centre. (CFFC boundary condition)

Fig 14 shows the longitudinal x-direction component (A_x), y-direction component (A_y), transverse component (A_z) of magnetic vector potential and the electric potential (ϕ) when sensor is placed at the centre with CFFC boundary condition. The longitudinal x-direction response is out of phase for $v_f = 0.6$ where as the longitudinal y-direction response is out of phase for both $v_f = 0.4$ and $v_f = 0.6$ compared to other volume fractions of the composite. The transverse direction component of magnetic potential is high for $v_f = 0.2$ of the composite.

e. FCFC boundary condition of the plate

Sensor near the edge

Fig 15 shows the longitudinal x-direction component (A_x), y-direction component (A_y), transverse component (A_z) of magnetic vector potential and the electric potential (ϕ) when sensor is placed near the edge with FCFC boundary condition. Volume fraction v_f *=0.4* having maximum piezoelectric coupling constant gives noticeably higher values of magnetic potential in the longitudinal x- direction, y-direction and the transverse direction. It is interesting to notice that volume fraction v_f *=1.0* which is a pure piezoelectric composite is giving equally good electric response as v_f *=0.2* when the sensor is placed near the edge of a FCFC plate.

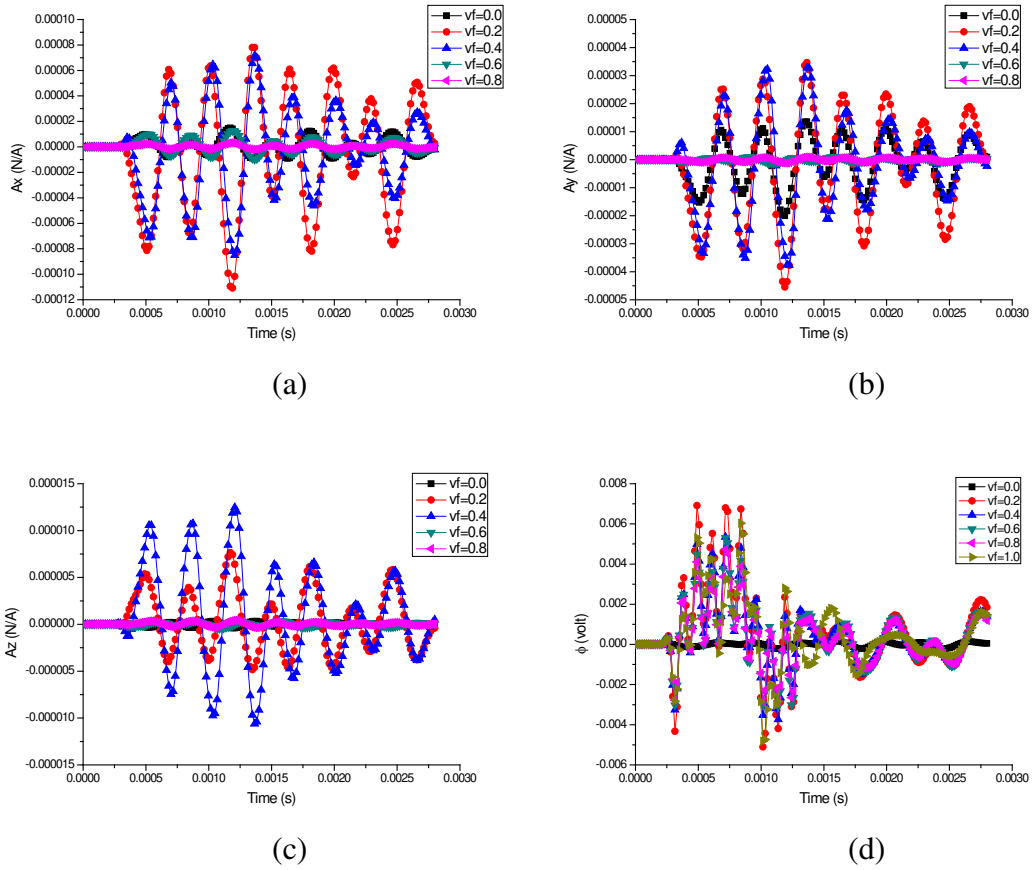

Fig 15 (a) Longitudinal x-direction component (A_x) (b) y-direction component (A_y), (c) transverse component (A_z) of magnetic vector potential and (d) electric potential (ϕ) when sensor is placed near the edge. (FCFC boundary condition)

Sensor at an off set of 0.075m

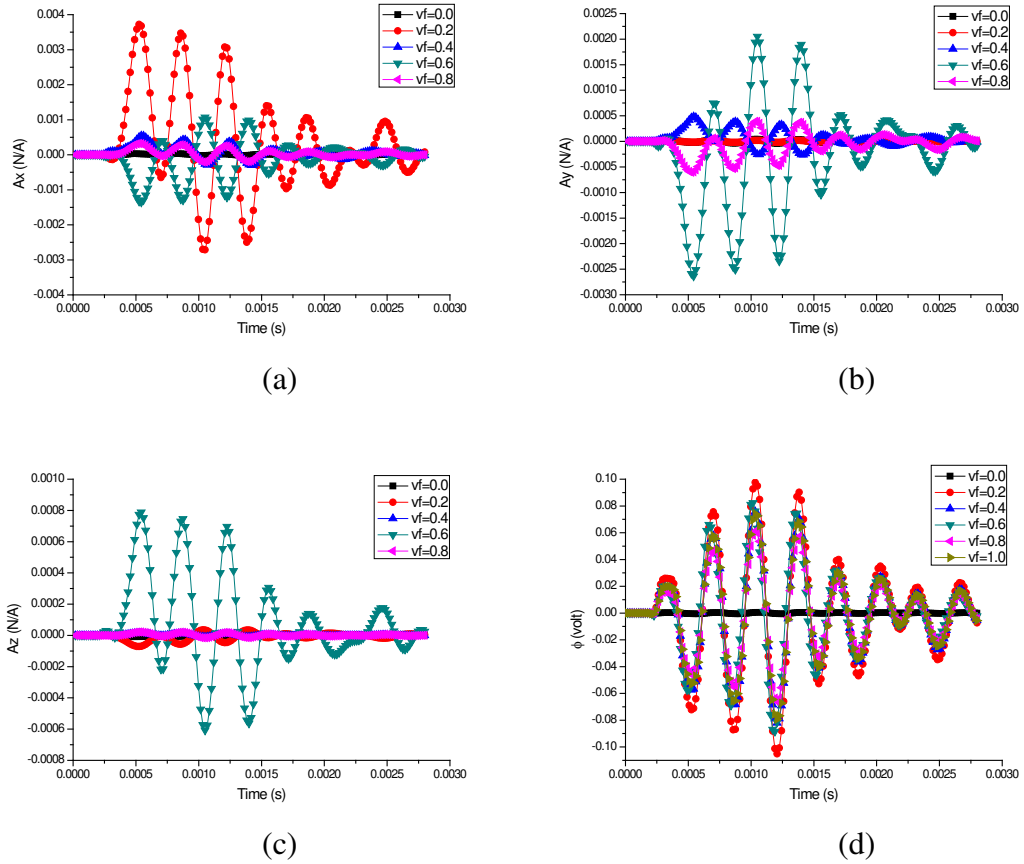

Fig 16 (a) Longitudinal x-direction component (A_x) (b) y-direction component (A_y), (c) transverse component (A_z) of magnetic vector potential and (d) electric potential (ϕ) when sensor is placed at an off set of 0.075m. (FCFC boundary condition)

The longitudinal x-direction component (A_x), y-direction component (A_y), transverse component (A_z) of magnetic vector potential and the electric potential (ϕ) when the sensor is placed at an off set of 0.075m from the edge with FCFC boundary condition is shown in Fig 16. Volume fraction v_f =*0.2* gives noticeably higher values of magnetic potential in longitudinal x- direction where as in the longitudinal y-direction and transverse direction, magnetic response is high for volume fraction v_f =*0.6*.

Sensor at the centre

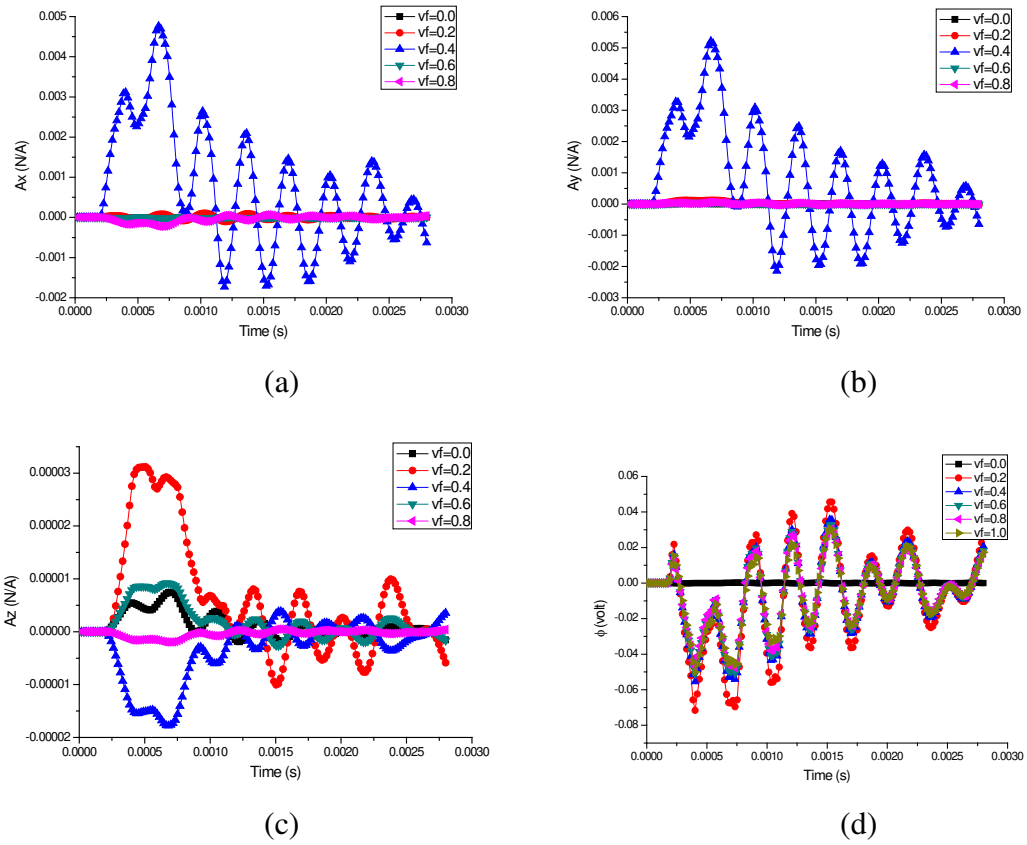

Fig 17 (a) Longitudinal x-direction component (A_x) (b) y-direction component (A_y), (c) transverse component (A_z) of magnetic vector potential and (d) electric potential (ϕ) when sensor is placed at the centre. (FCFC boundary condition)

Fig 17 shows the longitudinal x-direction component (A_x), y-direction component (A_y), transverse component (A_z) of magnetic vector potential and the electric potential (ϕ) when sensor is placed at the centre with FCFC boundary condition. Volume fraction v_f *=0.4* having high value of magneto electric coupling constant in the polarization direction gives noticeably higher values of magnetic potential in the longitudinal x-direction and y-direction. The transverse direction component of magnetic potential is maximum for volume fraction v_f *=0.2* and out of phase for v_f *=0.4*.

Table 2 Maximum electrical potential generated by the sensor for different boundary conditions and sensor locations.

Sensor Location	Boundary condition of the Base Plate			
	CCCC	**CCCF**	**CFFC**	**FCFC**
Near edge	0.025V	0.015V	0.060V	0.007V
Off set of 0.075m	0.070V	0.050V	0.015V	0.100V
Centre	0.060V	0.050V	0.025V	0.050V

A comparison of the maximum electrical potential generated for different sensor locations with the base plate subjected different boundary conditions is shown in Table 2. It is seen that the maximum electric potential is generated for FCFC boundary condition with the sensor located at an off set distance of 0.075m from the edge of the plate. The minimum electric potential is also for the same boundary condition with the sensor located near the edge of the plate.

IV CONCLUSIONS

Transient dynamic behavior of magneto-electro-elastic sensor bonded at various locations on a mild steel plate subjected to different boundary conditions is studied. The electric and magnetic response of the sensor for three sensor locations: near the edge, an off set of 0.075m from the edge and at the centre on the plate subjected to different boundary conditions (CCCC, CCCF, CFFC and FCFC) is investigated. It is seen that the electric response is maximum when volume fraction $v_f=0.2$ for all sensor locations with different boundary conditions which can be attributed to the induced strain because of the high elastic constants for $v_f=0.2$. The boundary conditions significantly influence the magnetic response of different volume fractions of the composite. Volume fraction $v_f=0.4$ gives noticeably higher values of magnetic potential in almost all the cases (except for CFFC boundary condition with sensor near the edge and FCFC boundary condition with sensor at an off set of 0.075m from the edge) which can be attributed to high value of magneto electric coupling constant in the polarization direction. The sensor magnetic response is noisy for volume fraction $v_f=0.2$ during the initial transient owing to the noisy electric response during that period for CFFC boundary condition with sensor at an off set of 0.075m from the edge. The decay in response is very slow for CFFC boundary condition with sensor at

the centre due to the influence of higher harmonics. These studies will be bench mark solutions in size, shape and location optimization of magneto-electro-elastic sensors and actuators during active vibration control.

REFERENCES

[1] G. R. Buchanan, Layered versus multiphase magneto-electro-elastic composites, Composites Part B, Vol. 35, 2004, pp. 413-420.

[2] J. Aboudi, Micromechanical analysis of fully coupled electro-magneto-thermo-elastic multiphase composites, Smart Materials and Structures, Vol.10, 2001, pp. 867-877.

[3] H. Huang Jin and Yu Heng-I, Dynamic electromechanical response of piezoelectric plates as sensors or actuators, Materials Letters, Vol. 46, 2000, pp. 70–80.

[4] Qing Guanghui, Qiu Jiajun and Liu Yanhong **,** A semi-analytical solution for static and dynamic analysis of plates with piezoelectric patches, International Journal of Solids and Structures, Vol. 43, 2006, pp. 1388–1403.

[5] M. Sunar, Ahmed Z. Al-Garni, M. H. Ali and R. Kahraman **,** Finite Element modeling of thermopiezomagnetic smart structures, AIAA Journal, Vol. 40, 2002, pp.1846-1851.

[6] J. Sirohi and I. Copra, Fundamental understanding of piezoelectric strain sensors, Journal of Intelligent Systems and Structures, Vol.11, 2000, pp. 246-257.

[7] H. Huang Jin and Yu Heng-I, Dymamic electromechanical response of piezoelectric plates as sensors and actuators, Material Letters, Vol. 46, 2000, pp. 70-80.

[8] D. P. Ghosh and S. Gopalakrishnan, Coupled analysis of composite laminate with embedded magnetostrictive patches Smart Materials and Structures, Vol. 14, 2005, pp.1462-1473.

[9] Galopin Nocolas, Mininger Xavier, Bouillault Frederic and Daniel Laurent, Finite Element modeling of magnetoelectric sensors, IEEE transactions on Magnetics, Vol. 44,2008, pp. 834-837.

[10] Pietrzakowski Marek, Piezoelectric control of composite plate vibration: Effect of electric potential distribution, Computers and Structures, Vol. 86, 2008, pp. 948-954.

[11] Daga Atul, N. Ganesan and K. Shankar, Behaviour of magneto-electro-elastic sensors under transient mechanical loading, Sensors and Actuators A: Physical, Vol. 150, 2009, pp. 46-55.

[12] X. Mininger, N.Galopin, Y. Dennemont and F.Bouillault, 3D finite element model for Magnetoelectric sensors, The Europian Physics journal, Vol. 52, 2010, pp. 23303–23307.

[13] Wang Ruifeng, Han Qingkai and E.Pan, Transient response of a bi-layered multiferroic composite plate, Acta Mechanica Solida Sinica, Vol. 24, 2011, pp. 83-91.

[14] B.Biju, N.Ganesan and K.Shankar, Dynamic response of multiphase Magneto-electro-elastic sensors using 3D Magnetic vector potential approach, IEEE sensor journal, Vol.11, 2011, pp. 2169-2176

[14] Chen Jiangyi, E.Pan and Chen Hualing, Wave propagation in magneto-electro-elastic multilayered plates, International journal of Solids and Structures, Vol. 44, 2007, pp. 1073-1085.